Chemistry & Biology
Article

Identification of an Allosteric Pocket on Human Hsp70 Reveals a Mode of Inhibition of This Therapeutically Important Protein

Anna Rodina,[1,6] Pallav D. Patel,[1,2,6] Yanlong Kang,[1,6,7] Yogita Patel,[3,6] Imad Baaklini,[3] Michael J.H. Wong,[3] Tony Taldone,[1] Pengrong Yan,[1] Chenghua Yang,[1] Ronnie Maharaj,[1] Alexander Gozman,[1,8] Maulik R. Patel,[1] Hardik J. Patel,[1] William Chirico,[4] Hediye Erdjument-Bromage,[5] Tanaji T. Talele,[2] Jason C. Young,[3,*] and Gabriela Chiosis[1,*]

[1]Program in Molecular Pharmacology and Chemistry and Department of Medicine, Memorial Sloan-Kettering Cancer Center, New York, NY 10021, USA
[2]Department of Pharmaceutical Sciences, College of Pharmacy and Allied Health Professions, St. John's University, 8000 Utopia Parkway, Queens, NY 11439, USA
[3]Department of Biochemistry, Groupe de Recherche Axé sur la Structure des Protéines, McGill University, Montreal, QC H3G 0B1, Canada
[4]Department of Cell Biology, SUNY Downstate Medical Center, Brooklyn, NY 11203, USA
[5]Program in Molecular Biology, Memorial Sloan-Kettering Cancer Center, New York, NY 10021, USA
[6]These authors contributed equally to this work
[7]Present address: BioZone Pharmaceuticals, Inc., 710 Fox Run Drive, Plainsboro, NJ 08536, USA
[8]Present address: UT Southwestern Medical Center, 5323 Harry Hines Boulevard, Dallas, TX 75390, USA
*Correspondence: jason.young2@mcgill.ca (J.C.Y.), chiosisg@mskcc.org (G.C.)
http://dx.doi.org/10.1016/j.chembiol.2013.10.008

SUMMARY

Hsp70s are important cancer chaperones that act upstream of Hsp90 and exhibit independent anti-apoptotic activities. To develop chemical tools for the study of human Hsp70, we developed a homology model that unveils a previously unknown allosteric site located in the nucleotide binding domain of Hsp70. Combining structure-based design and phenotypic testing, we discovered a previously unknown inhibitor of this site, YK5. In cancer cells, this compound is a potent and selective binder of the cytosolic but not the organellar human Hsp70s and has biological activity partly by interfering with the formation of active oncogenic Hsp70/Hsp90/client protein complexes. YK5 is a small molecule inhibitor rationally designed to interact with an allosteric pocket of Hsp70 and represents a previously unknown chemical tool to investigate cellular mechanisms associated with Hsp70.

INTRODUCTION

The 70 kDa heat shock proteins (Hsp70s) are ubiquitously found in many different species and are central components of the cellular network of molecular chaperones (Mayer and Bukau, 2005). In humans, there are at least 13 isoforms of Hsp70 located in all major cellular compartments, among which are two major cytoplasmic forms, the constitutive heat shock cognate 70 (Hsc70) and the inducible Hsp70 (Daugaard et al., 2007). Hsp70s are important regulators of the apoptotic machinery, including the apoptosome, the caspase activation complex, and apoptosis-inducing factor (AIF), and play a role in the proteasome-mediated degradation of apoptosis-regulating proteins. Hsp70s also participate in oncogenesis, as suggested by their constituency in the Hsp90 super-chaperone machinery, whereby the HSP-organizing protein (HOP) co-chaperone bridges the Hsp70 and the Hsp90 systems (Brodsky and Chiosis, 2006; Powers et al., 2010; Rérole et al., 2011). Thus, the downregulation or selective inhibition of Hsp70s might constitute a valuable strategy for the treatment of cancer, and be especially effective in overcoming tumor cell resistance (Brodsky and Chiosis, 2006; Patury et al., 2009; Powers et al., 2010; Rérole et al., 2011). Considering the importance of Hsp70 as a potential therapeutic target, several efforts centered on the discovery of small molecule Hsp70 inhibitors; however, only a limited number of molecules are available (Patury et al., 2009; Powers et al., 2010; Rérole et al., 2011).

The human Hsp70 (hHsp70) chaperones, Hsp70 and Hsc70, are composed of two major domains: an ~45 kDa, nucleotide binding domain (NBD) that contains the regulatory ATP/ADP binding pocket and an ~25 kDa substrate binding domain (SBD) joined together by a flexible linker (Mayer and Bukau, 2005). Nucleotide binding and hydrolysis and communication between the two domains are essential for Hsp70 molecular chaperone activity; thus, it is not surprising that the few known Hsp70 modulators interfere either with nucleotide binding and/or with the conformational motility of the protein. A few of these compounds, such as 15-deoxyspergualin, pifithrin-μ (2-phenylethynesulfonamide), a small molecular weight peptide (NRLLLTG), and fatty acid acyl benzamides, are believed to bind to the SBD of Hsp70 while dihydropyrimidines and myricetin to its NBD (Haney et al., 2009; Patury et al., 2009; Powers et al., 2010; Rérole et al., 2011). However, little, if any, structural information on these complexes is available. Recently, adenosine-based analogs were designed to bind within the ATPase pocket of Hsp70 (Williamson et al., 2009). All of these compounds have been used in cellular models of disease to investigate mechanisms associated with Hsp70, in spite of their low

potency and pleiotropic effects on cells that are little known (Powers et al., 2010; Rérole et al., 2011), underscoring the need for better Hsp70 inhibitor-based chemical tools.

Our preferred approach for the identification of small molecule inhibitors is one that combines structure-based design with phenotypic assays (Chiosis et al., 2001; He et al., 2006). For Hsp70 however, although several high-resolution crystal and solution structures are available for Hsp70s of several species (Flaherty et al., 1994; Kityk et al., 2012; Sriram et al., 1997; Wisniewska et al., 2010; Worrall and Walkinshaw, 2007; Zhu et al., 1996), a crystal structure of a functionally intact hHsp70 chaperone containing both NBD and SBD has not been resolved. Furthermore, while several crystal structures are available for the human NBD, most capture it in a relatively closed conformation (Sriram et al., 1997; Wisniewska et al., 2010). In contrast, recent nuclear magnetic resonance (NMR) techniques and molecular dynamics studies suggest considerable flexibility and rearrangements in this domain with the cleft opening upon ADP binding (Bhattacharya et al., 2009; Woo et al., 2009). Thus for flexible proteins such as Hsp70, where ligand binding pockets are influenced by global protein conformational changes, X-ray structures may not properly capture all potentially available ligand binding sites.

We here build a theoretical model for hHsp70 that allows for the discovery of a druggable allosteric pocket and the rational design of small molecules that selectively occupy this pocket. We demonstrate that the identified small molecules inhibit the biological functions of human Hsp70 in cells and are valuable tools for parsing out mechanisms associated with Hsp70.

RESULTS AND DISCUSSION

Modeling Leads to a Structure of Full-Length Human Hsp70

Lacking a structure of hHsp70 optimal for our ligand discovery efforts, we first sought to construct a homology model (a theoretical three-dimensional structure) for full-length hHsp70 that captures the conformational flexibility of the protein. The most important factors in homology model construction are correctness of alignment and the choice of template structures (Wallner and Elofsson, 2005). The N-terminal crystal structure of the hHsp70 protein (Protein Data Bank [PDB] ID: 1S3X; Sriram et al., 1997) was the best available template for the amino acids in this region of Hsp70 (Met1-Gly382, hHsp70). No crystal structure was available for the hHsp70 SBD, therefore the *Escherichia coli* Hsp70 (DnaK) structure (PDB ID: 2KHO; Bertelsen et al., 2009), a protein that shares a 62% similarity with hHsp70, was selected as a template for modeling a segment of the SBD (Asp385-Gln538, *E. coli.*; Asp383-Ala541, hHsp70). Finally, the crystal structure of *Caenorhabditis elegans* Hsp70 (PDB ID: 2P32; Worrall and Walkinshaw, 2007) was used as a template for the C terminus (Leu543-Ser614, *C. elegans*; Leu542-Gly613, hHsp70). The extreme C-terminal amino acids (614–641) of hHsp70 did not have a template structure, and hence were not modeled. After template selection, alignment of the template and the ability to detect the structural similarities based on the amino acid sequence, determine the overall quality of the model. For closely related protein sequences with high similarity, the alignment is most often optimal. In our study, 606 of 613 residues were identical to the three implemented templates (PDB ID: 1S3X, 2KHO, and 2P32), indicating optimal alignment (Figure S1A available online). Following alignment of the residue side chains, amino acids missing in the template structure (PDB ID: 2KHO), such as Lys384, Ser385, Glu386, Asn387, and Arg509 (hHsp70), were successfully inserted using a semi-automated procedure in Prime. The model thus obtained contained loops based on the template structure (excluding termini). All the loop regions (33 loops) were optimized using the loop refinement tool in Prime to generate proper conformations for loops. Finally, the obtained protein model was subjected to a protein preparation utility, followed by rigorous energy minimization to relax unfavorable contacts. Superimposition of the backbone atoms in the NBD of the homology model and the template structure (PDB ID: 1S3X) gave a root-mean-square deviation of 1.01 Å and a good alignment score of 0.05 (smaller is better, more than one poor alignment), validating our model (Figure S1B). The homology model thus contained 613 amino acid residues and had two major domains, an NBD and an SBD, joined together by a flexible linker (Figure 1A). The N-terminal ATPase domain displayed an actin-like hexokinase fold and had two globular lobes, I (subdomains IA and IB) and II (subdomains IIA and IIB). Twelve α helices and 16 β sheets compiled the NBD, which corroborates with the crystal structure of the NBD (Sriram et al., 1997). The C-terminal SBD contained two functionally relevant subdomains; a sandwich of two four-stranded β sheets containing the peptide binding subdomain (SBD-β) and a four α helix subdomain (SBD-α), also called the lid domain (Zhu et al., 1996).

This nucleotide-free structure of hHsp70 was then superimposed with approximately 25 structures of Hsp70 resolved by crystallography. These were resolved for Hsp70 paralogs from different species, including the human protein, and captured the protein in the apo-, the ATP-, or the ADP-bound state (http://www.rcsb.org). Our model most closely resembles that of the ADP-bound Hsp70, with the distinction that the model captures the N-terminal binding cleft in a conformation that is more open than that seen in the X-ray determined structure (Figures S1B and S1C). As indicated by NMR techniques and molecular dynamics, Hsp70 is a flexible protein in which several residues rotate and move substantially during chaperone cycling. During these conformational movements, several energetically favored minima are possible. The energy minimization simulation protocol that we used in creating the homology model sampled several such possible dynamic conformations and identified the captured conformation, energetically as a preferred conformation. Crystal structures also capture a specific energetic minimum, which, possibly influenced by the crystallization conditions, differs from that captured by our computations, providing a possible explanation to the differences in Hsp70 structure captured by crystallography and the computational modeling.

Modeling Unveils Five Druggable Sites in hHsp70

The quality of any homology model depends on the force field and the sampling procedure. Although Prime, the software used in our simulations, uses an improved energy model (Li et al., 2011), our derived structure may, nonetheless, deviate from the native structure at any location in the protein. In spite of these potential limitations, we used the theoretical model to

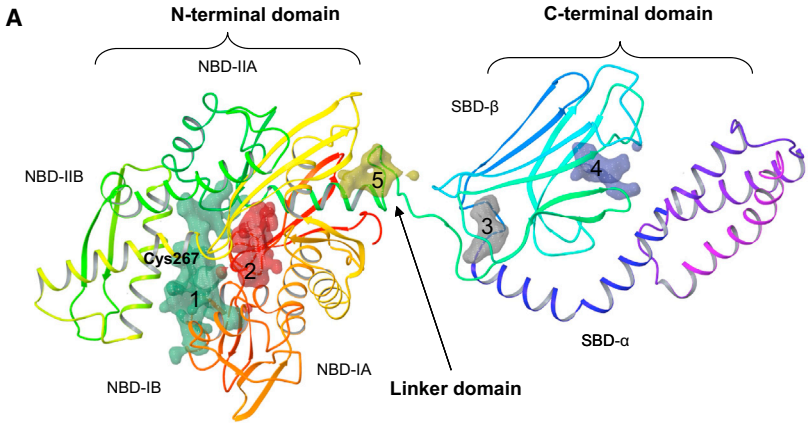

B

Binding Site	Position	S-score	D-score	Size	G-score[a]
Site 1	IB and IIB	1.05	1.00	365	-7.66
Site 2	IA and IIA	1.12	0.91	178	-3.61
Site 3	SBD-β	1.06	0.98	95	-2.04
Site 4	SBD-β and SBD-α	0.94	0.97	83	-2.73
Site 5	Linker domain	0.78	0.71	51	-2.59

[a] SP G-score expressed as kcal/mol is obtained by docking YK5 on individual sites and a more negative G-score indicates a better fit in the binding site.

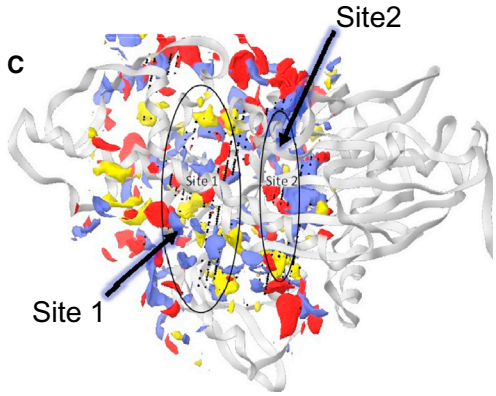

Figure 1. Building of the hHsp70 Homology Model and Evaluation of the Potential Druggable Sites

(A) Secondary structure of the homology model of hHsp70. The position and geometry of various "sites" generated by SiteMap on the hHsp70 homology model are shown.

(B) Characteristics of the five binding sites as calculated by SiteMap and Glide docking.

(C) Hydrophobic/hydrophilic maps of site 1 and site 2 are shown as determined by SiteMap. Hydrophobic, hydrogen bond donor, and hydrogen bond acceptor maps are shown in yellow, blue, and red, respectively. For clarity, only the N-terminal region of hHsp70 homology model is displayed.

See also Figure S1.

identify sites for the design of Hsp70 inhibitors using SiteMap. This software considers several physical descriptors such as size, degree of enclosure/exposure, tightness, van der Waals forces, hydrophobic/hydrophilic character, and hydrogen-bonding possibilities to find potential ligand-binding pockets. It does so by linking together site points that are most likely to contribute to protein/ligand or protein/protein interaction. After it examines the entire structure, it then ranks the sites. The size of the site (measured by the number of found site points), the relative openness of the site (measured by the exposure and enclosure properties), and tightness of the site (measured by the contact term and the hydrophobic and hydrophilic character of the site) contribute significantly toward ranking. The top five sites scored by SiteMap had a Site-score (S-score) of ~0.80 or higher (Figure 1B) and thus these could be plausible ligand-binding sites (Halgren, 2009). Other sites, scoring lower than 0.8, such as those on the protein surfaces, were potential artifacts of the computational model and eliminated from further analysis.

In addition to the S-score, we also measured in SiteMap the druggability of the site, as described by the D-score (Figure 1B). The D-score includes terms that promote ligand binding, such as adequate size and isolation from solvents, but offsets them with a term that penalizes increasing hydrophilicity. With use of the D-score criteria, sites are classified into undruggable, difficult to drug, and druggable (Halgren, 2009). Undruggable sites are strongly hydrophilic, relatively smaller in size, with little or no hydrophobic character, and are characterized by a D-score value lower than 0.83 (site 5, Figure 1B). Difficult sites are sufficiently hydrophilic to require administration as a prodrug, but they are less hydrophobic than a typical binding site and are defined by a D-score value between 0.83 and 0.98 (sites 2–4, Figure 1B). Druggable sites are of a size, enclosure, hydrophobicity, and hydrophilicity to favorably accommodate a small molecule ligand, and, moreover, hold a D-score value higher than 0.98 (site 1, Figure 1B).

Among the best five predicted sites, sites 3, 4, and 5 had a limited number of site points (described by size in Figure 1B), the cavity was small and the site shallow (Figure 1A). As a result, it is more difficult to generate sufficient binding affinity for these sites. Site 2, including the groove occupied by the endogenous ligands ATP and ADP, had a favorable size (site points: 178; Figure 1B) and S-score (1.12; Figure 1B). On closer inspection, site 2 mainly consisted of hydrophilic amino acids (Figure 1C). In the absence of suitable regions for hydrophobic interactions, it was potentially more difficult to target, as depicted by its D-score (0.91, Figure 1B). This site is also conserved in the actin fold family of ATPases that consists of Hsp70, actin, and sugar kinases,

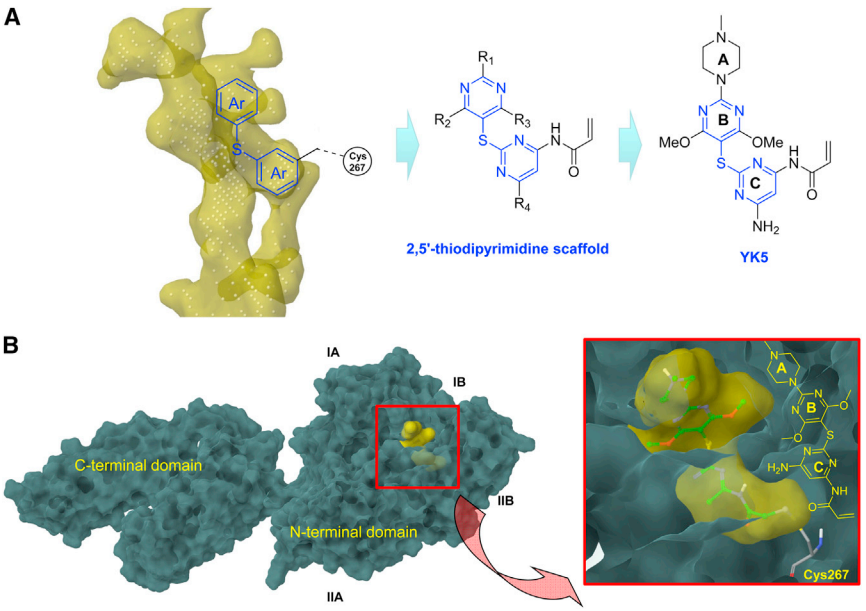

Figure 2. Design of Site 1 Interacting Small Molecules and Computational Validation of Their Binding Mode

(A) General structure of the 2,5′-thiodipyrimidine scaffold and of the lead derivative, YK5, designed to properly fit into site 1 (yellow surface). The compounds also incorporate the acrylamide group for potential interaction with Cys267 located in site 1.

(B) Surface model representation of the best Glide-predicted binding pose derived for compound YK5 within the allosteric site 1.

See also Figures S1 and S2.

and a high structural homology in the ATP domain exists between these proteins (Sriram et al., 1997), altogether rendering this pocket less desirable for ligand design.

Homology Model Unveils a Drugabble Site Not Evident in X-Ray Structures

Site 1, located in a cleft region outside the ATP/ADP binding domain (Figure 1A) and flanked by subregions IB and IIB, was larger in size (site points: 385; Figure 1B), had a larger groove and consisted of hydrophilic and hydrophobic amino acids, suggesting this site as most druggable on hHsp70 (D-score: 1.00; S-score: 1.05; Figure 1B). Hydrophobic/hydrophilic maps also indicated site 1 to be of a favorable character for ligand design being lined by a balanced number of hydrophilic and hydrophobic residues, such as Tyr41, Val59, Phe68, Asp69, His89, Pro91, Glu231, Asp234, Val238, Val260, Arg261, Leu263, and Arg264 (numbering as in human Hsp70) (Figure 1C).

As indicated above, the several available crystal structures of Hsp70 capture the nucleotide binding domain in a relatively closed conformation. Concordantly, a SiteMap analysis conducted on the X-ray structure of Hsp70 (PDB ID: 1S3X) indicated a smaller cavity for the allosteric site1 (Figures S1B and S1C), specifically of only 138 site points as compared to 385 site points in the homology model.

On further analysis, we noted that site 1 also contained a potentially reactive cysteine residue located at the base of the cavity (Figures 1A, S1B, and S1C; Cys267). Interestingly, whereas this Cys is captured in all available crystal structures buried inside the protein (Figures S1B and S1C), evidence suggests that conformational changes in Hsp70 that expose this residue do occur in the native protein (Liu et al., 1996; Miyata et al., 2012).

Taking together the S- and D-scores, its size, its balanced hydrophobic and hydrophilic character, exposure and enclosure properties, site 1 was predicted to be the most druggable cavity in Hsp70, and thus we focused on this allosteric site 1 for further design of Hsp70 inhibitors.

Rational Design Identifies Previously Unknown Allosteric Site Binders

Upon analysis of the size and geometry of site 1 (Figure 2A), we mentally designed several scaffolds that we predicted would adopt a proper conformation and would favorably interact with the allosteric structural groove of hHsp70 (Kang et al., 2012). We then positioned the acrylamide at one end of the molecule where it could form a potential covalent bond between the inhibitor and Cys267. Due to the location of Cys267 deep inside the cavity (Figures S1B and S1C), such bond formation would be possible only after the ligand inserted into the pocket and achieved a proper fit. By gaining affinity through a covalent linkage in addition to enthalpy, one can increase the ligand's apparent affinity for the protein even when its fit is less than optimal. Thus, the use of this technique for early stage ligand design offers advantages, especially when the architecture of the binding pocket, as captured by the homology model may not entirely capture the native pocket. We reasoned that once a proper scaffold for this pocket was identified, we could improve the enthalpy of binding through medicinal chemistry efforts, eliminating the need for the covalent bond.

With this method, we designed and synthesized several scaffolds, one being based on 2,5′-thiodipyrimidines (termed YK-class, Figure 2A). It is noteworthy that these compounds are of a chemical space yet little explored by either nature or man. From these efforts, we identified a lead compound, YK5 that we will analyze here.

Computational Analysis Predicts Favorable Binding of YK5 to Hsp70

To investigate the binding of YK5 to Hsp70, we first performed a computational analysis. Binding interactions, compound orientation (Figure 2B), and G-score values concluded that YK5 bound most favorably into site 1. The best binding mode derived by docking of YK5 onto site 1 showed the piperazine (ring A) pointing toward the exit and the acrylamide toward the bottom of the pocket (Figure 2B). Modeling predicted several favorable interactions between site 1 and YK5 (Figure S2A). Specifically, the alkene group of the acrylamide moiety was favorably placed to form a covalent adduct with Cys267 (distance of 2.6 Å between the alkene and the sulfur) and to establish hydrophobic interactions with Leu237 and Val238 (~3 Å). Other interactions of the acrylamide and surrounding residues (i.e., Arg264, Glu268) are also possible. The 6-NH_2 on

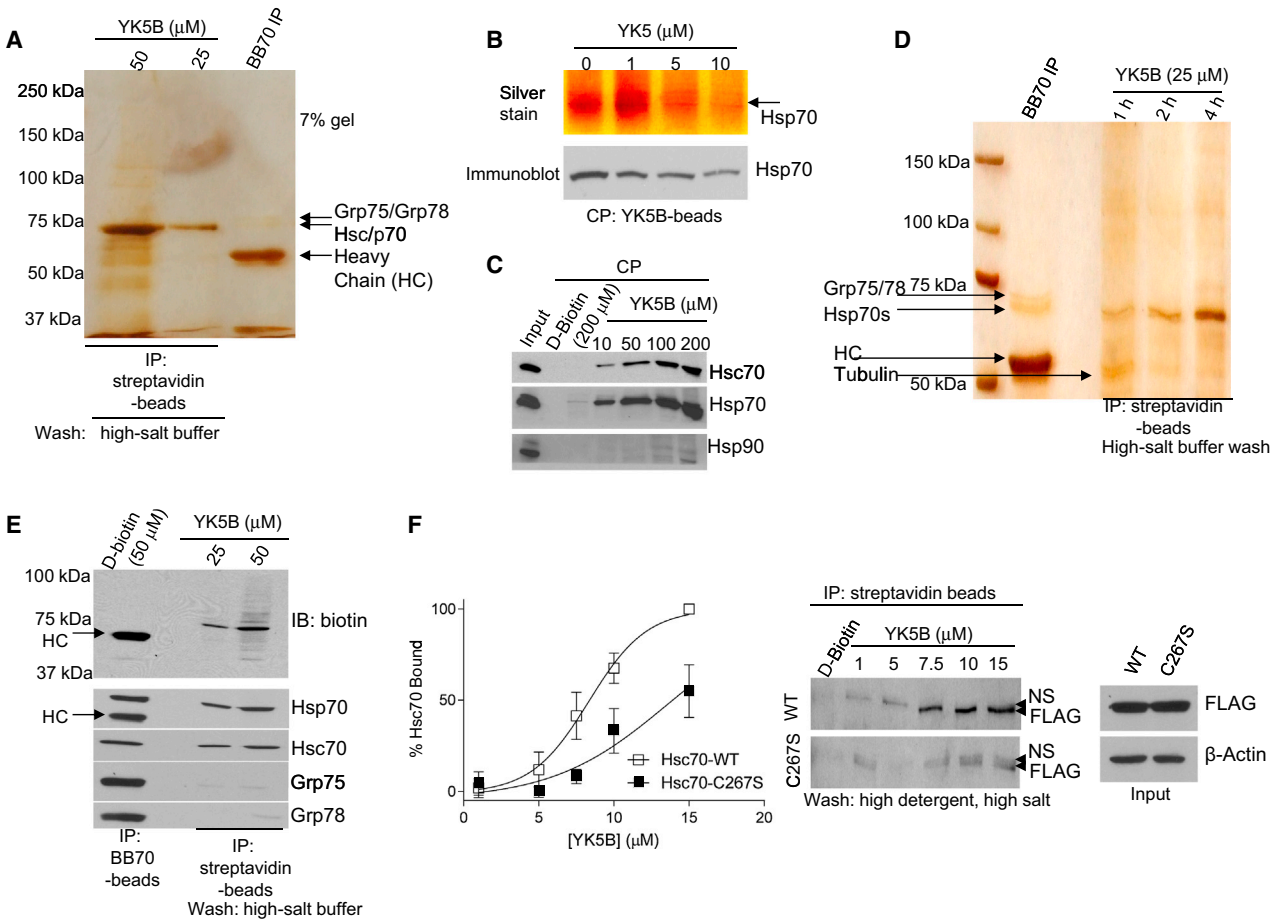

Figure 3. YK5 Interacts Selectively with the Cytosolic Hsp70 and Hsc70 through the Allosteric Site 1

(A) Cancer cells were treated with the indicated concentrations of YK5-biotin (YK5B) for 6 hr prior to lysing and precipitation of protein complexes on streptavidin beads. Beads were washed with high-salt (1 M NaCl) buffer, proteins eluted by boiling in 2% SDS, separated on a denaturing gel, and silver stained. BB70 Ab pull-downs were used to indicate the position of Hsp70s (BB70 IP). This antibody recognizes Hsp70, Hsc70, Grp75, and Grp78. This experiment was repeated twice with comparable results.

(B) Cancer cells were treated for 24 hr with the indicated concentrations of YK5 and cells were lysed. Protein complexes were isolated through chemical precipitation by incubating the cell extract with YK5B-beads, eluted with 2%SDS, separated on a denaturing gel, and depicted as indicated.

(C) Protein complexes from cancer cell extracts were isolated through chemical precipitation with YK5B-beads or an inert molecule, D-biotin. Proteins were then separated on a denaturing gel and analyzed with western blot (WB). This experiment was repeated twice with comparable results.

(D) Cancer cells were treated for the indicated times with YK5B, prior to lysing and precipitation of protein complexes on streptavidin beads. Beads were washed with high-salt buffer, proteins eluted by boiling in 2% SDS, separated on a denaturing gel, and silver stained.

(E) The experimental set-up was similar to that in (A), but proteins were analyzed with WB.

(F) Experiment set-up as in (A) for cancer cells transfected with FLAG-tagged Hsc70-wild-type or Hsc70-C267S and incubated with YK5B for 4 hr. Beads were washed with high salt/high detergent (RIPA with 1M NaCl) before WB analysis. The amount of Hsc70 remaining on the YK5B-beads was quantified and then plotted against the concentration of YK5B. Data are presented as mean ± SD (n = 5). A representative WB is also shown (right).

See also Figures S3–S5.

ring C is poised for ionic interactions with the carboxylate group of Asp234 and Glu268, whereas ring C may be stabilized by cation-π interactions with the guanidine group of Arg264. The piperazine of YK5 is poised to form hydrogen bonds with the backbone -C = O of His89. We also designed a negative control compound, YK20 (Figure S2B), to use for further testing.

Biochemical Analyses Validate that YK5 Interacts Selectively with Hsp70

To experimentally confirm our computational prediction that YK5 interacted with hHsp70 at the allosteric site, we designed a biotinylated YK5 derivative, YK5-biotin (YK5B; Kang et al., 2012). The addition of YK5B (Figure 3A) but not of D-biotin to cancer cells, followed by isolation of complexes on streptavidin beads and washing of beads with high-salt buffer, identified a major band around 70 kDa, which was competed off in a dose-dependent manner by cell pretreatment with soluble YK5 (Figure 3B). We used an anti-Hsp70 antibody BB70 as a positive control (Figure 3A; BB70 IP).

There are at least eight highly homologous Hsp70 family members, including the constitutively expressed Hsc70, several inducible forms including Hsp70-1 and Hsp70-6, all mainly

localized in the cytosol, and the mitochondrial and the endoplasmic reticulum forms, Grp75 and Grp78, respectively (Daugaard et al., 2007). Liquid chromatography-tandem mass spectroscopy (LC/MS-MS) analysis of peptide digests obtained from the YK5B-isolated band confirmed the presence of two inducible Hsp70 isoforms (Hsp70-1 and Hsp70-6), and of Hsc70, the constitutive Hsp70 member (Hsp70-8; Table S1A), all three cytosolic Hsp70 members. Their identity was further investigated by western blot, to demonstrate Hsc70 and Hsp70 but not the unrelated chaperone, Hsp90, in the YK5B-pulldowns (Figure 3C).

Together these findings confirm that, when exposed to a complex protein mixture such as that present in the cancer cell, YK5 selectively and tightly binds to the cytosolic Hsp70s.

YK5 Interacts with the Allosteric Site 1 of Hsp70

We next demonstrated interaction of YK5 with the allosteric site 1 and potential covalent bond formation between YK5 and Hsp70 upon binding. For compounds where irreversible binding plays a role, the half-maximal inhibitory concentration (IC_{50}) consists of two components, one reflecting reversible binding and another reflecting the subsequent covalent binding, and depends on the extent to which the covalent interaction has occurred. Indeed, incubation of cells for 1–4 hours with YK5B but not D-biotin led to a progressive increase in the amount of immobilized 70 kDa band (Figure 3D), which by anti-biotin and Hsp70 immunoblots (Figure 3E), was suggested to be an YK5B-Hsp70-containing species. Weak to no interaction of YK5B with Grp75 and Grp78, the mitochondrial and the endoplasmic reticulum Hsp70 family members, respectively, was detected under these conditions by silver stain (Figure 3D) and immunoblot (Figure 3E), confirming the LC/MS-MS findings (Table S1A).

Elution of protein complexes from the YK5B-beads in conditions sufficiently harsh to disrupt the tightest known noncovalent binding, the streptavidin-biotin complex (Rösli et al., 2008), confirmed that a covalently bound YK5-Hsp70 species was formed when cells were incubated with YK5 (Figure S3). Trypsin digestion of the YK5B-bound Hsp70s species, but not of BB70 antibody pulldowns, identified a major m/z peak at 1867.915 atomic mass units that corresponds to YK5B attached to LRTAC^{267}ERAK (Figure S4). No labeling of these peptides was observed when YK5B-Hsp70 isolates were reduced and nonspecifically alkylated on remaining cysteines using beta-mercaptoethanol and acrylamide, respectively (Table S1B). The TACERAK sequence is conserved in human cytosolic Hsp70s, but divergent in Grp75 and Grp78 (Figure S5), consistent with their lack of interaction with YK5B under similar conditions (Figures 3D and 3E; Table S1). Furthermore, high salt, high detergent conditions eluted preferentially the Hsc70-C267S protein over the WT form from preformed Hsc70/YK5B complexes (Figure 3F).

Collectively, these data confirm interaction of YK5 with site 1, as predicted by molecular modeling. They also indicate that the interaction of YK5 with Hsp70 and Hsc70 consists of two elements, one reflecting reversible binding of favorable enthalpy and another subsequent covalent cysteine modification. There is precedent for the use of an acrylamide "warhead" in the development of irreversible inhibitors for kinases (i.e., epidermal growth factor receptor [EGFR], receptor tyrosine-protein kinase erbB-2 and -4 [HER2 and HER4], and B cell progenitor kinase), that like Hsp70s, contain a reactive cysteine in their regulatory site. These inhibitors, such as neratinib, dacomitinib, afatinib, and PCI-32765, are in advanced clinical trials for cancer (Singh et al., 2011).

YK5 Inhibits the Biochemical Functions of Hsp70

Next, we investigated whether binding of YK5 to Hsp70 interfered with its main biochemical activities, specifically refolding of a denatured client protein and its ATPase activity (Figure 4). Hsp70 activities are stimulated by Hsp40 proteins and nucleotide exchange factors, such as Hsp110 (Mayer and Bukau, 2005; Wegele et al., 2004; Young et al., 2004). Humans have several cytosolic Hsp40s, including Hdj1, DJA1, DJA2, and DJA4, and we have recently reported that DJA1 provides the strongest stimulation of Hsc70 ATPase activity, whereas DJA2 is most efficient in promoting the refolding of an Hsc70/Hsp70 polypeptide substrate, firefly luciferase (Baaklini et al., 2012; Bhangoo et al., 2007; Tzankov et al., 2008).

YK5 dose-dependently inhibited the refolding of luciferase by purified Hsc70 and DJA2 (Figure 4A). In cells, the refolding of heat-denatured luciferase by endogenous as well as transfected Hsp70 was inhibited by YK5. The nonspecific capacity of transfected Hsp70 to maintain substrate solubility after heat shock was not greatly affected, indicating that YK5 targeted the specific substrate folding activity of Hsp70 (Figure 4B). YK5 also inhibited Hsc70, whereas Hsp70-C267S gained resistance (Figure 4B). YK5 had no effect on the DJA1-stimulated ATPase rate of recombinant Hsc70, and only partially inhibited the ATPase rate stimulated by DJA1 and Hsp110 (Figure 4C). Because the YK5 binding site does not overlap with that of ATP, its effect probably results from disruption of the coordination of the N- and C-terminal domains essential for chaperone function. The modest defect in nucleotide exchange assisted by Hsp110 may be a secondary effect of disrupted coordination. In the in vitro reconstituted systems, the core biochemical functions of Hsp70 were inhibited by YK5 in assay conditions that do not favor covalent bond formation, further indicating, in addition to covalent reactivity, an appropriate fit for YK5 in the active site of the target, as computationally predicted. Indeed, subsequent medicinal chemistry on YK5 resulted in reversible Hsc70 and Hsp70 binders of low nanomolar activity (Kang et al., 2012 and G.C., unpublished data).

YK5 Inhibits the Functions of Hsp70 in Cancer Cells

Having demonstrated that YK5 is a specific Hsp70s interactor and because Hsp70s are important regulators of Hsp90 tumor activity (Moulick et al., 2011; Workman et al., 2007), we next investigated if YK5 inhibited the Hsp70/Hsp90-pathway in cancer cells. Hsp90 in concert with Hsc70, the constitutive and Hsp70, the inducible Hsp70 isoforms, maintains the transforming capacity of several oncoproteins, including HER2, Akt, Raf-1, insulin-like growth factor-I receptor, and hypoxia-inducible factor 1; Brodsky and Chiosis 2006; Daugaard et al., 2007; Rérole et al., 2011; Workman et al., 2007).

As evidenced in the SKBr3 breast cancer cells, YK5, but not the negative control derivative YK20, induced the degradation of HER2, Raf-1, and Akt kinases (Figure 5A), all three of which are known Hsp90/Hsp70 complex onco-client proteins in this

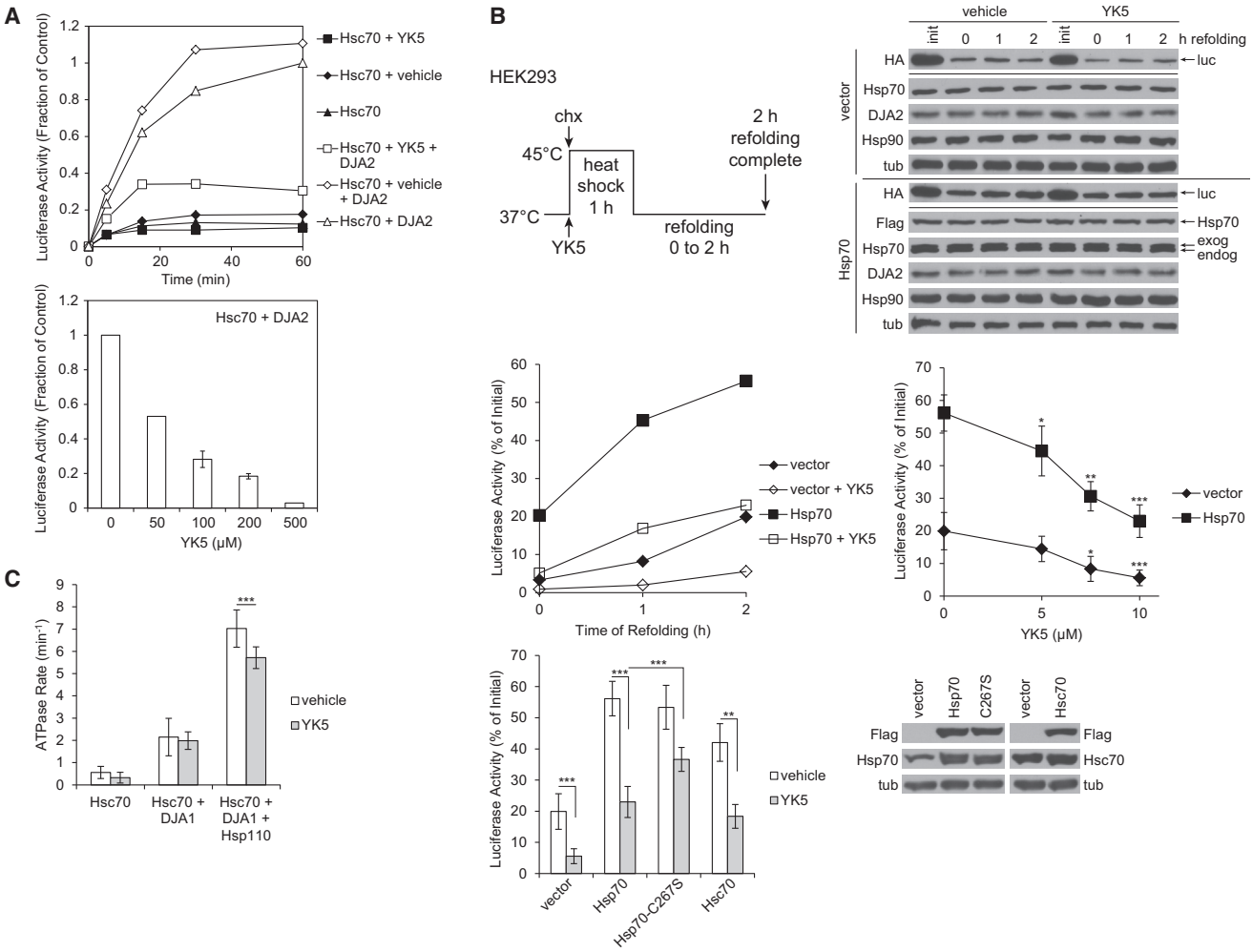

Figure 4. YK5 Inhibits the Core Biochemical Functions of hHsp70

(A) Refolding of guanidinium-HCl denatured luciferase by Hsc70 and DJA2 at 30°C was measured for the indicated times in the presence of YK5 (100 μM) or vehicle (above), or at 60 min in the presence of indicated concentrations of YK5 (below). In this and all graphs, errors bars represent SDs from the mean of multiple independent experiments ($n \geq 4$), *$p < 0.05$, **$p < 0.01$, ***$p < 0.001$.

(B) HEK293 cells were transfected with luciferase and either control vector, Hsp70, Hsp70-C267S, or Hsc70. The cells were treated with cycloheximide and either vehicle or YK5 at 10 μM unless otherwise indicated, incubated at 45°C for 1 hr, and allowed to recover at 37°C for 2 hr (left). Cells were lysed during and after refolding, and soluble HA-tagged luciferase and chaperones were detected in the lysates; exogenous transfected Flag-tagged Hsp70 and Hsc70 are visible as bands above endogenous Hsp70 and Hsc70 (right). Luciferase enzymatic activities in the lysates were measured at 2 hr of refolding, unless otherwise indicated, and represented as percentages of the initial activity before heat shock (below). YK5 inhibited endogenous Hsp70, and transfected Hsp70 and Hsc70, $p < 0.001$, $p < 0.001$, and $p = 0.0018$, respectively, in multiple experiments ($n \geq 5$). The YK5 IC_{50} for luciferase refolding in cells is ~7 μM. The activity of Hsp70 was not significantly different from that of Hsp70-C267S ($p = 0.315$), but Hsp70-C267S was less inhibited by YK5 relative to wild-type ($p < 0.001$).

(C) Hsc70 ATPase rates were measured for reactions at 30°C with the indicated combinations of Hsc70 and co-chaperones in the presence of vehicle (DMSO) or YK5 (100 μM). ADP production was monitored with thin-layer chromatography separation of radiolabeled ADP from ATP and phosphorimaging analysis. YK5 had little effect on the basal Hsc70 ATPase rate or the DJA1-stimulated rate but inhibited the DJA1- and Hsp110-stimulated rate, $p = 0.081$, 0.587 and $p < 0.001$, respectively.

See also Figure S6.

cellular context (Chiosis et al., 2001). Furthermore, the nononcogenic tyrosine-protein kinase CSK, a c-Src related tyrosine kinase, remained unaffected by the YK-agents and the direct Hsp90 inhibitor PU-H71 (He et al., 2006; Figure 5A). YK5 also induced apoptosis in these cells as evidenced by PARP cleavage (Figure 5A; cPARP).

These effects were not mediated by direct Hsp90 inhibition. Only inhibitors of Hsp90 such as PU-H71 and PU24FCl (Vilenchik et al., 2004), but not YK5, competed with a fluorescently labeled Hsp90 ligand, GM-Cy3B (Moulick et al., 2006), for Hsp90 binding (Figure 5B). Moreover, YK5B failed to bind Hsp90 in experimental conditions it substantially isolated Hsp70 from cancer cells extracts (Figure 3C).

In the SKBr3 breast cancer cells, degradation of Hsp90/Hsp70-onco-client proteins by YK5 occurred at the increasing low micromolar concentrations that also led to inhibition of cell

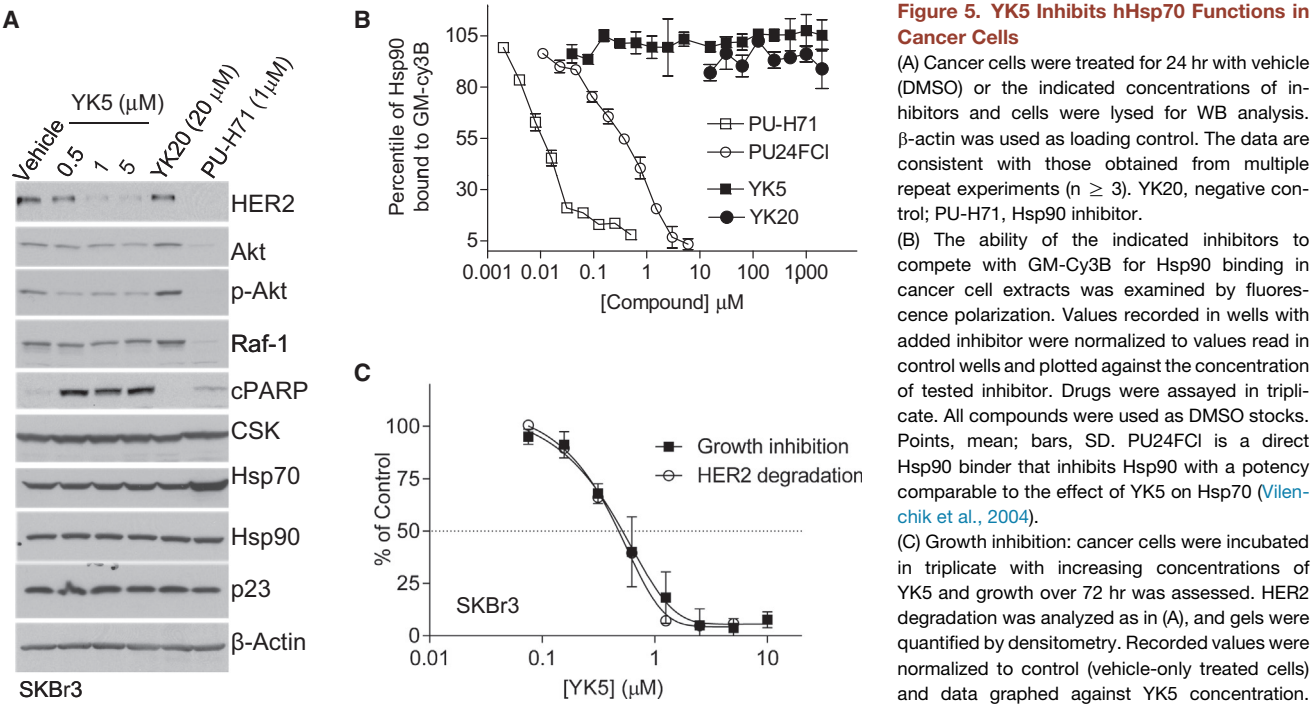

Figure 5. YK5 Inhibits hHsp70 Functions in Cancer Cells

(A) Cancer cells were treated for 24 hr with vehicle (DMSO) or the indicated concentrations of inhibitors and cells were lysed for WB analysis. β-actin was used as loading control. The data are consistent with those obtained from multiple repeat experiments (n ≥ 3). YK20, negative control; PU-H71, Hsp90 inhibitor.

(B) The ability of the indicated inhibitors to compete with GM-Cy3B for Hsp90 binding in cancer cell extracts was examined by fluorescence polarization. Values recorded in wells with added inhibitor were normalized to values read in control wells and plotted against the concentration of tested inhibitor. Drugs were assayed in triplicate. All compounds were used as DMSO stocks. Points, mean; bars, SD. PU24FCl is a direct Hsp90 binder that inhibits Hsp90 with a potency comparable to the effect of YK5 on Hsp70 (Vilenchik et al., 2004).

(C) Growth inhibition: cancer cells were incubated in triplicate with increasing concentrations of YK5 and growth over 72 hr was assessed. HER2 degradation was analyzed as in (A), and gels were quantified by densitometry. Recorded values were normalized to control (vehicle-only treated cells) and data graphed against YK5 concentration. Error bars represent the SD of the mean (n = 3).

proliferation (Figure 5C). Collectively, the concordance in the observed biochemical (Figure 4B) and phenotypic (Figure 5) effects observed with YK5 in cancer cells suggest that, in the tested concentration range, the biological activity of YK5 is majorly and selectively channeled through its Hsp70-binding mechanism.

YK5 Alters the Hsp90/Hsp70 Machinery

We next investigated the mechanisms by which YK5 exerted its biological activity. The function of the Hsp90 protein complex requires the HSP-organizing protein (HOP), involved in the formation of the intermediate chaperone complex where client is bound to both Hsp70 and Hsp90 and others, such as p23, that act at the final or mature Hsp90 complex (Workman et al., 2007). Treatment of cells with YK5 altered the formation of the Hsp90-HOP-Hsp70 complex, but not the Hsp90-p23 complexes (Figure 6A). This effect occurred at concentrations in accord with its observed biological effect (compare Figure 6B with Figure 5). It also resulted in onco-proteins release from Hsp90 (i.e., Raf-1; Figure 6C) associated with a time-dependent reduction in their steady-state levels (Figure 6D). The mechanism of degradation of these onco-proteins by YK5 was associated with protein destabilization and cell clearance acceleration, as demonstrated by reduced protein half-life (Figure 6E). Consistent with a pathway of degradation via the proteasome, and further confirmatory of an Hsp70/Hsp90 complex-mediated effect, inhibitors of the proteasome but not of other proteolytic enzymes efficiently rescued their degradation by YK5 (Figure 6F).

Collectively, these results indicate that the biological effects of YK5 in cancer cells are, at least in part, mediated by altering the formation of a functional Hsp90 multi-chaperone machinery (Figure 6G). When Hsp70 is inhibited by YK5, Hsp90 machinery onco-proteins cannot be transferred onto Hsp90, become destabilized and targeted for clearance, at least in part by the proteasome.

The Effect of YK5 on Hsp90 Is Uncoupled from HSF-1

The transcription factor heat shock factor-1 (HSF-1), the master regulator of heat shock response, is another Hsp90 client, and unlike onco-proteins, it becomes activated when Hsp90 is inhibited (Workman et al., 2007; Zou et al., 1998). HSF-1 activation leads to a feedback increase in Hsp70 levels. Because, Hsp70 in itself is a powerful anti-apoptotic molecule that inhibits both intrinsic and extrinsic apoptotic pathways (Brodsky and Chiosis 2006; Rérole et al., 2011), this feedback response limits the potency of Hsp90 inhibitors (Bagatell et al., 2000). In fact, the anti-apoptotic function of Hsp70 is not limited to Hsp90 inhibitors, and in general, Hsp70 protects cells from many other apoptotic and necrotic stimuli (Daugaard et al., 2007; Rérole et al., 2011).

Feedback induction of Hsp70 was undetected with YK5 at concentrations and in the time interval where we observed its effects on Hsp90 onco-clients (Figure 7A). Meanwhile, in these cells, direct Hsp90 inhibitors potently activated a heat shock response, as evidenced by Hsp70 induction (Figure 7A; PU24FCl).

We next investigated the mechanism behind this effect. HSF-1 regulation by Hsp90 is mediated by formation of an Hsp90-HSF-1 complex that maintains the transcription factor in a monomeric state. Upon exposure of cells to an Hsp90 inhibitor, the chaperone dissociates from HSF-1, permitting it to trimerize, enter the nucleus, and bind to heat shock response elements found in the promoters of heat shock proteins, including Hsp70 (Zou et al., 1998). YK5 had no effect on HSF-1 activation (Figure 7B). Only heat shock and direct Hsp90 inhibitors (i.e., PU24FCl), but

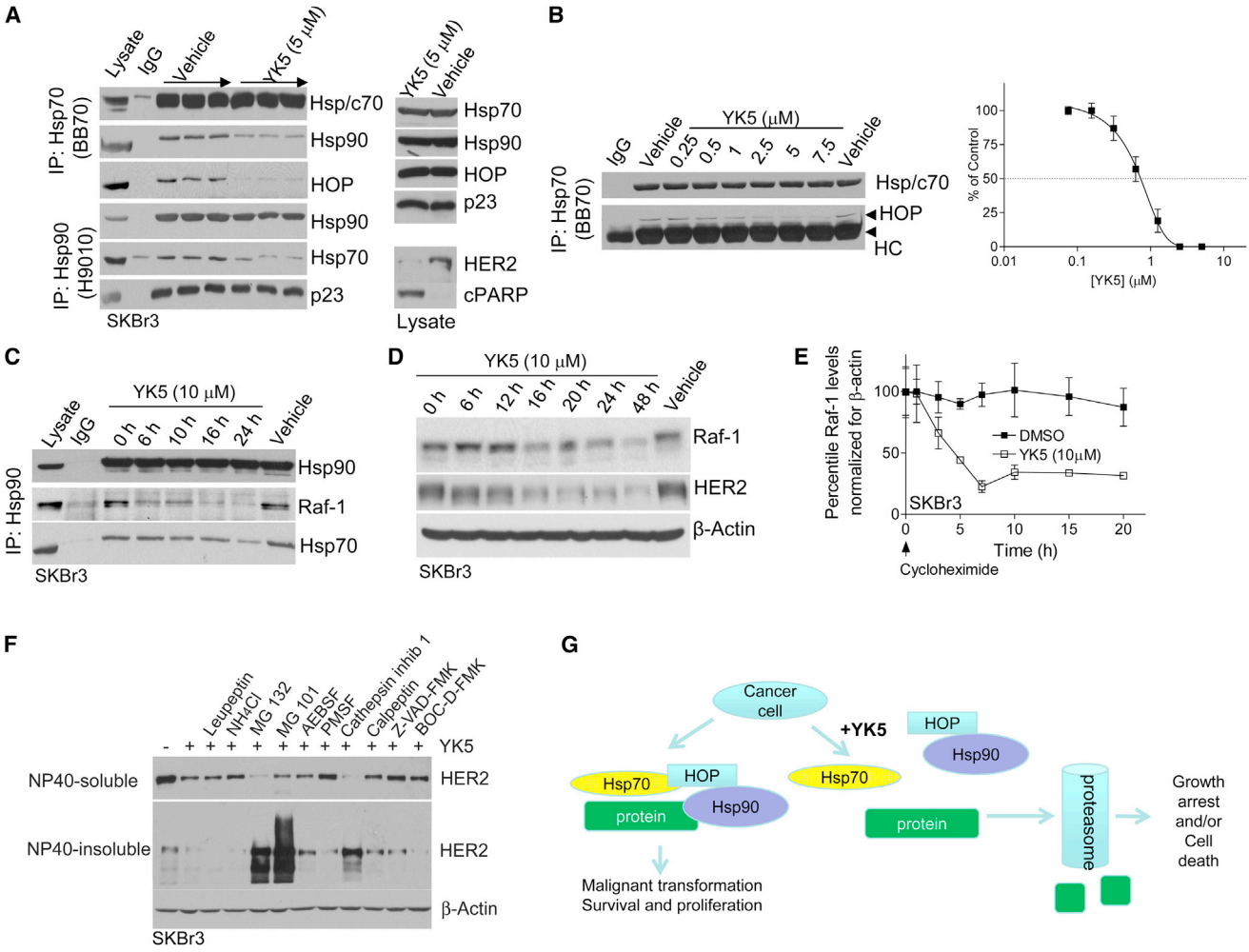

Figure 6. Addition of YK5 to Cancer Cells Leads to Disruption of the Hsp90 Onco-Protein Regulating Machinery

(A–C) Cancer cells were treated for 24 hr with vehicle or indicated concentrations of YK5 (A and B) or for the indicated times with YK5 (C). Proteins isolated with anti-Hsp90 and Hsp70s antibodies (IP: Hsp90 or Hsp70), or present in the cell extract (lysate) were analyzed with WB. Specificity of binding was tested with a control IgG. HC, heavy chain. For (B), gels were quantified with densitometry and recorded values were normalized to control (vehicle-only treated cells) and data were graphed against the YK5 concentration. Error bars represent the SD of the mean (n = 3).

(D) Representative WB of cancer cells treated for the indicated times with YK5. β-actin, loading control. This experiment was repeated twice with comparable results.

(E) Cancer cells were treated for the indicated times with the protein biosynthesis inhibitor cycloheximide in the presence of vehicle (DMSO) or YK5 (10 μM). Following WB analysis, protein expression was quantified by densitometry and graphed against time of treatment. Points, mean; bars, SD.

(F) Cancer cells were pretreated with the indicated proteolysis machinery inhibitors prior to addition of YK5 (10 μM). MG132 (Z-LL-CHO) and MG101 are proteasome inhibitors. After 24 hr of treatment, protein expression in both detergent-soluble and insoluble fractions, in the presence (F) and absence of YK5 (not shown) were analyzed with WB.

(G) Proposed mechanism of action for YK5 for altering the cancer-promoting Hsp90 machinery. The Hsp90 chaperoning cycle is a dynamic process in which onco-client proteins are processed through an intermediate complex containing Hsp90, Hsp70, and HOP, leading to the conformational maturation of the onco-protein, and cell proliferation and survival. YK5, by inhibiting Hsp70, interferes with the formation of a competent chaperone/onco-client complex, resulting in onco-protein destabilization and its consequent clearance by the proteasome. This leads to cancer cell growth arrest and death.

not YK5, led to the formation of HSF-1 trimers, a process required for HSF-1 activation and nuclear translocation. Potentially as a consequence of this difference in their mechanism of action, YK5, but not PU24FCl and PU-H71, led to substantial apoptosis in these cells, as evidenced by cleavage of PARP (Figures 5A and 7A; cPARP).

These findings conclude that the onco-protein regulatory action of the Hsp90 machinery can be differentiated from its effects on HSF-1 by upstream Hsp70 and Hsc70 inhibition by YK5. In this regard, YK5 becomes a chemical tool to study the biological effect of Hsp90 machinery inhibition in a chemical-HSF-1 knockdown environment. The advantages of this intervention are evident over the genetic manipulations of HSF-1, allowing for temporal and spatial analysis of the cellular environment.

YK5′s Binding Mode Is Distinct from That of Myricetin

We next investigated whether the phenotype observed with YK5 could be recapitulated with another Hsp70 binder, myricetin

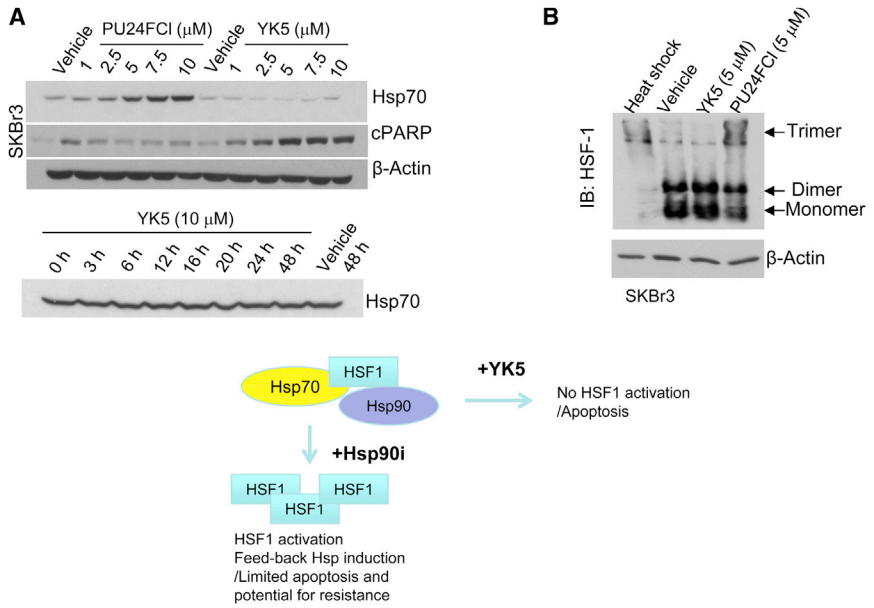

Figure 7. YK5 Leads to No HSF-1 Activation or Feedback Heat Shock Response in Cancer Cells

(A) Cancer cells were treated for 24 hr with vehicle or indicated concentrations of inhibitors or for the indicated times with YK5. Proteins were analyzed with WB. β-actin, loading control. cPARP; cleaved PARP. These experiments were repeated three times with comparable results.

(B) Cancer cells were heat shocked for 45 min at 42°C or incubated with vehicle, YK5, or PU24FCI for 3 hr. Proteins were applied to a native gel and analyzed with immunoblotting. This experiment was repeated twice with comparable results.

(Figure S6). This compound was recently reported to interact with a site potentially adjacent to that occupied by YK5 (Chang et al., 2011). In this report, myricetin binding to the *E. coli* Hsp70, DnaK, a protein that lacks Cys267 (is Ala266 in DnaK), was analyzed. Upon inspection of the proposed binding mode of myricetin and YK5, we note that while there are a few residues in common, the two agents are unlikely to occupy the same pocket (Figure S6A). Several residues reported to affect binding of myricetin to DnaK are more than 4 Å away from the site occupied by YK5. Furthermore, myricetin effectively inhibited the ATPase activity of DnaK (Chang et al., 2011) and the DJA2-stimulated ATPase of Hsc70, unlike YK5 (Figures 4C and S6B). When tested in several of our biochemical and cellular assays, myricetin failed to mimic the phenotype we observe with YK5. Specifically, although myricetin impaired in vitro luciferase refolding, it had no effect on luciferase refolding activity in cells (Figure S6B), marginally altered the Hsp70-HOP complex in cells (Figure S6C), and failed to degrade Raf-1 or induce apoptosis in SKBr3 cells (Figure S6D). It is possible that for myricetin its lack of activity in cells is due to a very low stability, as suggested previously by others. Indeed, when we performed a time-dependent analysis of this agent with LC/MS-MS, we could not detect myricetin in cells as early as 10 min following its addition.

Altogether, these findings indicate that distinct Hsp70 inhibitors may result in nonoverlapping phenotypes and underscore the need for the discovery of Hsp70 ligands that act on the protein at discrete sites and/or through diverse mechanisms.

SIGNIFICANCE

Our study uncovers a therapeutically viable allosteric binding site in hHsp70 that allows for the design of a potent and selective inhibitor, YK5. This pocket and its interaction mode with YK5 are not obvious nor entirely predicted by any of the available crystal structures, because they capture a binding domain with the Cys267 unexposed to the solvent. We also provide chemical tools, such as YK5 and a biotinylated YK5, to investigate Hsp70s in endogenous cellular systems where the proteins are limiting but not absent. We assembled these chemical entities through rational design. We believe these tools will allow for the identification of novel mechanisms for this therapeutically important chaperone protein and will provide valuable starting points for the discovery of clinically relevant drugs that act through such mechanism. While there is a concern that an acrylamide entity could indiscriminately react with nontarget-related proteins resulting in pleiotropic effects, incubation of cells with YK5 concentrations five to ten times higher than those needed to inhibit Hsp70 cellular activity in cancer cells resulted selectively in the formation of YK5-Hsp70 adducts. In addition, agents that result in unspecific oxidation and labeling of cysteines are known to increase cellular protein misfolding and to lead to consequent protective activation of a heat shock response, phenomenon not observed with YK5. At the physiologically relevant concentration of 10 μM (i.e., needed to maximally inhibit Hsp70-cancer functions), YK5 was also inert when tested against Ambit's 402 kinase panel (G.C., unpublished data). Indeed, further studies in this class demonstrated that reversible inhibitors designed around YK5 retained an Hsp70-mediated mechanism, indicating that the acrylamide group could be eliminated altogether by improving the enthalpy of the binding. These findings confirm that at the tested concentrations, YK5 is a specific Hsp70 and Hsc70 dual modulator, and thus, an appropriate tool to dissect the significance of pharmacologic Hsp70s inhibition in cellular systems.

EXPERIMENTAL PROCEDURES

Reagents

We synthesized and characterized PU24FCI and PU-H71 as previously described (He et al., 2006; Vilenchik et al., 2004). The synthesis and characterization of YK5 and YK5B is described elsewhere (Kang et al., 2012). We purchased leupeptin, MG 132, MG 101, and PMSF from Sigma-Aldrich; AEBSF from A.G. Scientific; and Z-VAD-FMK, BOC-D-FMK, cathepsin inhibitor 1, and calpeptin from Calbiochem.

Buffers

We used high-salt buffer (20 mM Tris pH 7.4, 1 M NaCl, and 0.1% NP-40), low-salt buffer (20 mM Tris pH 7.4, 25 mM NaCl, and 0.1% NP-40 buffer), or high

salt/high detergent (50 mM Tris, pH 7.4, 1% NP-40, 0.25% Na- deoxycholate, 1 M NaCl, and 1 mM EDTA) as indicated. To elute protein complexes from YK5B-beads, we used, as indicated, either elution buffer A (62.5 mM TrisHCl pH 6.8, 2% SDS, 10% glycerol, 15.5 mg/ml dithiothreitol, and bromophenol blue 0.02 mg/ml) and boiled the sample at 100°C for 3 min or elution buffer B (2% SDS, 50 mM phosphate, 100 mM NaCl, 6 M urea, and 2 mM thiourea) and incubated the sample for 15 min at room temperature, followed by 15 min at 100°C.

Cell Lines

SKBr3 cells were a gift from Dr. Neal Rosen, Memorial Sloan-Kettering Cancer Center while K562 cells were obtained from American Type Culture Collection and were cultured routinely in DME/F12 (SKBr3) or in RPMI (K562) supplemented with 10% fetal bovine serum, 1% L-glutamine, 1% penicillin, and streptomycin.

Covalent Binding

K562 cells were treated with the indicated amount of YK5B for the indicated time. Cells were collected and lysed in 20 mM Tris pH 7.4, 25 mM NaCl, and 0.1% NP-40 buffer. Cell extract (500 μg) in 100 μl of the lysis buffer was incubated with streptavidin agarose beads for 1 hr at 4°C. Samples were washed five times with the lysis buffer or high salt (20 mM Tris pH 7.4, 1 M NaCl, and 0.1% NP-40) buffer and subjected to SDS-PAGE. Gels were silver stained according to the manufacturer's procedure (Invitrogen) or proteins were transferred onto nitrocellulose membrane followed by immunoblotting.

Chemical Precipitation

Protein lysates were prepared using 20 mM Tris pH 7.4, 25 mM NaCl, and 0.1% NP-40 lysis buffer. Streptavidin agarose beads (50 μl; Thermo Scientific) were washed three times with lysis buffer, YK5B was added at the indicated concentrations and the complexes were incubated at 4°C for 1 hr. Upon a three-time wash with buffer, beads were added to the indicated amount of total cellular protein in buffer. Samples were incubated at 4°C overnight, washed five times with the lysis buffer, and applied to SDS-PAGE.

Immunoprecipitation

Cells were collected and lysed in 20 mM Tris pH 7.4, 25 mM NaCl, and 0.1% NP-40 buffer. Each sample contained 500 μg of a total protein. Appropriate antibody (BB70 for Hsp70 and H9010 for Hsp90; 5 μl) or normal IgG (5 μl; as a negative control) was added to each sample together with protein G agarose beads (30 μl; Upstate) and incubated at 4°C overnight. Samples were washed five times with lysis buffer, and applied on SDS-PAGE followed by a standard western blotting procedure.

Hsp70/HOP Complex Analysis

SKBr3 cells were treated with the indicated concentrations of the inhibitor for 24 hr. Samples were collected and lysed in 20 mM Tris pH 7.4, 25 mM NaCl, and 0.1% NP-40 buffer with protease inhibitors added. Aliquots of 500 μg of total protein adjusted to 100 μl with the lysis buffer were prepared. Samples were incubated with 5 μl of BB70 antibody (Stressmarq) or normal IgG (as a negative control) and 20 μl of protein G agarose beads (Upstate) at 4°C overnight. Samples were washed five times with the lysis buffer, and applied on SDS-PAGE followed by a standard western blotting procedure to detect levels of HOP protein in the Hsp/c70 complexes upon treatment.

More methods detailing analyses of proteasome-mediated degradation, cycloheximide treatments, western blotting, native gel electrophoresis, biochemical analyses of Hsp70 ATPase activity and luciferase refolding, Hsp90 binding, and transfection studies are found in the Supplemental Experimental Procedures.

Modeling

Computational studies were conducted using the Schroedinger Suite (http://www.schrodinger.com). Details on the homology model building, binding site prediction, and ligand docking techniques are summarized in the Supplemental Experimental Procedures.

Mass Spectrometry

Protein identification was performed by the Proteomics Core of MSKCC and methods are detailed in the Supplemental Experimental Procedures.

SUPPLEMENTAL INFORMATION

Supplemental Information includes Supplemental Experimental Procedures, Figures S1–S6, and Table S1 and can be found with this article online at http://dx.doi.org/10.1016/j.chembiol.2013.10.008.

ACKNOWLEDGMENTS

The authors are supported in part by the Department of Defense (to T.T.), the MSKCC Technology Development Fund (to G.C.), the SPORE Pilot Award and Research & Therapeutics Program in Prostate Cancer (to G.C.), the Byrne Fund (to G.C.), the Geoffrey Beene Cancer Research Center of MSKCC (to G.C.), the Breast Cancer Research Fund (to G.C.), NIH grant R01 CA119001 (to G.C.), Susan G. Komen for the Cure (to T.T.), the Canadian Institutes of Health Research (to J.C.Y.), and resources from the College of Pharmacy at St. John's University (to P.D.P.). G.C. is also supported by NIH grants 1U01AG32969-01A1, 1R01CA155226-01, 1R01 CA172546-01A1, and 1R21AI090501-01. We thank Dr. Tianzhu Zang (Northeastern University) for advice on tandem mass spectroscopy spectra interpretation. MSKCC holds the intellectual rights to the YK5-type Hsp70 inhibitors. Samus Therapeutics, of which G.C. has partial ownership, has licensed the associated composition of matter.

Received: April 26, 2013
Revised: September 19, 2013
Accepted: October 10, 2013
Published: November 14, 2013

REFERENCES

Baaklini, I., Wong, M.J., Hantouche, C., Patel, Y., Shrier, A., and Young, J.C. (2012). The DNAJA2 substrate release mechanism is essential for chaperone-mediated folding. J. Biol. Chem. *287*, 41939–41954.

Bagatell, R., Paine-Murrieta, G.D., Taylor, C.W., Pulcini, E.J., Akinaga, S., Benjamin, I.J., and Whitesell, L. (2000). Induction of a heat shock factor 1-dependent stress response alters the cytotoxic activity of hsp90-binding agents. Clin. Cancer Res. *6*, 3312–3318.

Bhangoo, M.K., Tzankov, S., Fan, A.C., Dejgaard, K., Thomas, D.Y., and Young, J.C. (2007). Multiple 40-kDa heat-shock protein chaperones function in Tom70-dependent mitochondrial import. Mol. Biol. Cell *18*, 3414–3428.

Bertelsen, E.B., Chang, L., Gestwicki, J.E., and Zuiderweg, E.R. (2009). Solution conformation of wild-type E. coli Hsp70 (DnaK) chaperone complexed with ADP and substrate. Proc. Natl. Acad. Sci. USA *106*, 8471–8476.

Bhattacharya, A., Kurochkin, A.V., Yip, G.N., Zhang, Y., Bertelsen, E.B., and Zuiderweg, E.R. (2009). Allostery in Hsp70 chaperones is transduced by subdomain rotations. J. Mol. Biol. *388*, 475–490.

Brodsky, J.L., and Chiosis, G. (2006). Hsp70 molecular chaperones: emerging roles in human disease and identification of small molecule modulators. Curr. Top. Med. Chem. *6*, 1215–1225.

Chang, L., Miyata, Y., Ung, P.M., Bertelsen, E.B., McQuade, T.J., Carlson, H.A., Zuiderweg, E.R., and Gestwicki, J.E. (2011). Chemical screens against a reconstituted multiprotein complex: myricetin blocks DnaJ regulation of DnaK through an allosteric mechanism. Chem. Biol. *18*, 210–221.

Chiosis, G., Timaul, M.N., Lucas, B., Munster, P.N., Zheng, F.F., Sepp-Lorenzino, L., and Rosen, N. (2001). A small molecule designed to bind to the adenine nucleotide pocket of Hsp90 causes Her2 degradation and the growth arrest and differentiation of breast cancer cells. Chem. Biol. *8*, 289–299.

Daugaard, M., Rohde, M., and Jäättelä, M. (2007). The heat shock protein 70 family: Highly homologous proteins with overlapping and distinct functions. FEBS Lett. *581*, 3702–3710.

Flaherty, K.M., Wilbanks, S.M., DeLuca-Flaherty, C., and McKay, D.B. (1994). Structural basis of the 70-kilodalton heat shock cognate protein ATP hydrolytic activity. II. Structure of the active site with ADP or ATP bound to wild type and mutant ATPase fragment. J. Biol. Chem. *269*, 12899–12907.

Halgren, T.A. (2009). Identifying and characterizing binding sites and assessing druggability. J. Chem. Inf. Model. *49*, 377–389.

Haney, C.M., Schneider, C., Beck, B., Brodsky, J.L., and Dömling, A. (2009). Identification of Hsp70 modulators through modeling of the substrate binding domain. Bioorg. Med. Chem. Lett. *19*, 3828–3831.

He, H., Zatorska, D., Kim, J., Aguirre, J., Llauger, L., She, Y., Wu, N., Immormino, R.M., Gewirth, D.T., and Chiosis, G. (2006). Identification of potent water soluble purine-scaffold inhibitors of the heat shock protein 90. J. Med. Chem. *49*, 381–390.

Kang, Y., Taldone, T., Rodina, A., Patel, P.D. and Chiosis, G. June 2012. Heat shock protein binding compounds, compositions, and methods for making and using same. U.S. patent EP2467142 A2.

Kityk, R., Kopp, J., Sinning, I., and Mayer, M.P. (2012). Structure and dynamics of the ATP-bound open conformation of Hsp70 chaperones. Mol. Cell *48*, 863–874.

Li, J., Abel, R., Zhu, K., Cao, Y., Zhao, S., and Friesner, R.A. (2011). The VSGB 2.0 model: a next generation energy model for high resolution protein structure modeling. Proteins *79*, 2794–2812.

Liu, Q., Levy, E.J., and Chirico, W.J. (1996). N-Ethylmaleimide inactivates a nucleotide-free Hsp70 molecular chaperone. J. Biol. Chem. *271*, 29937–29944.

Mayer, M.P., and Bukau, B. (2005). Hsp70 chaperones: cellular functions and molecular mechanism. Cell. Mol. Life Sci. *62*, 670–684.

Miyata, Y., Rauch, J.N., Jinwal, U.K., Thompson, A.D., Srinivasan, S., Dickey, C.A., and Gestwicki, J.E. (2012). Cysteine reactivity distinguishes redox sensing by the heat-inducible and constitutive forms of heat shock protein 70. Chem. Biol. *19*, 1391–1399.

Moulick, K., Clement, C.C., Aguirre, J., Kim, J., Kang, Y., Felts, S., and Chiosis, G. (2006). Synthesis of a red-shifted fluorescence polarization probe for Hsp90. Bioorg. Med. Chem. Lett. *16*, 4515–4518.

Moulick, K., Ahn, J.H., Zong, H., Rodina, A., Cerchietti, L., Gomes DaGama, E.M., Caldas-Lopes, E., Beebe, K., Perna, F., Hatzi, K., et al. (2011). Affinity-based proteomics reveal cancer-specific networks coordinated by Hsp90. Nat. Chem. Biol. *7*, 818–826.

Patury, S., Miyata, Y., and Gestwicki, J.E. (2009). Pharmacological targeting of the Hsp70 chaperone. Curr. Top. Med. Chem. *9*, 1337–1351.

Powers, M.V., Jones, K., Barillari, C., Westwood, I., van Montfort, R.L., and Workman, P. (2010). Targeting HSP70: the second potentially druggable heat shock protein and molecular chaperone? Cell Cycle *9*, 1542–1550.

Rérole, A.-L., Jego, G., and Garrido, C. (2011). Hsp70: anti-apoptotic and tumorigenic protein. Methods Mol. Biol. *787*, 205–230.

Rösli, C., Rybak, J.N., Neri, D., and Elia, G. (2008). Quantitative recovery of biotinylated proteins from streptavidin-based affinity chromatography resins. Methods Mol. Biol. *418*, 89–100.

Singh, J., Petter, R.C., Baillie, T.A., and Whitty, A. (2011). The resurgence of covalent drugs. Nat. Rev. Drug Discov. *10*, 307–317.

Sriram, M., Osipiuk, J., Freeman, B., Morimoto, R., and Joachimiak, A. (1997). Human Hsp70 molecular chaperone binds two calcium ions within the ATPase domain. Structure *5*, 403–414.

Tzankov, S., Wong, M.J.H., Shi, K., Nassif, C., and Young, J.C. (2008). Functional divergence between co-chaperones of Hsc70. J. Biol. Chem. *283*, 27100–27109.

Vilenchik, M., Solit, D., Basso, A., Huezo, H., Lucas, B., He, H., Rosen, N., Spampinato, C., Modrich, P., and Chiosis, G. (2004). Targeting wide-range oncogenic transformation via PU24FCl, a specific inhibitor of tumor Hsp90. Chem. Biol. *11*, 787–797.

Wegele, H., Müller, L., and Buchner, J. (2004). Hsp70 and Hsp90—a relay team for protein folding. Rev. Physiol. Biochem. Pharmacol. *151*, 1–44.

Williamson, D.S., Borgognoni, J., Clay, A., Daniels, Z., Dokurno, P., Drysdale, M.J., Foloppe, N., Francis, G.L., Graham, C.J., Howes, R., et al. (2009). Novel adenosine-derived inhibitors of 70 kDa heat shock protein, discovered through structure-based design. J. Med. Chem. *52*, 1510–1513.

Wisniewska, M., Karlberg, T., Lehtiö, L., Johansson, I., Kotenyova, T., Moche, M., and Schüler, H. (2010). Crystal structures of the ATPase domains of four human Hsp70 isoforms: HSPA1L/Hsp70-hom, HSPA2/Hsp70-2, HSPA6/Hsp70B', and HSPA5/BiP/GRP78. PLoS ONE *5*, e8625.

Wallner, B., and Elofsson, A. (2005). All are not equal: a benchmark of different homology modeling programs. Protein Sci. *14*, 1315–1327.

Woo, H.J., Jiang, J., Lafer, E.M., and Sousa, R. (2009). ATP-induced conformational changes in Hsp70: molecular dynamics and experimental validation of an in silico predicted conformation. Biochemistry *48*, 11470–11477.

Workman, P., Burrows, F., Neckers, L., and Rosen, N. (2007). Drugging the cancer chaperone HSP90: combinatorial therapeutic exploitation of oncogene addiction and tumor stress. Ann. N Y Acad. Sci. *1113*, 202–216.

Worrall, L.J., and Walkinshaw, M.D. (2007). Crystal structure of the C-terminal three-helix bundle subdomain of C. elegans Hsp70. Biochem. Biophys. Res. Commun. *357*, 105–110.

Young, J.C., Agashe, V.R., Siegers, K., and Hartl, F.U. (2004). Pathways of chaperone-mediated protein folding in the cytosol. Nat. Rev. Mol. Cell Biol. *5*, 781–791.

Zhu, X., Zhao, X., Burkholder, W.F., Gragerov, A., Ogata, C.M., Gottesman, M.E., and Hendrickson, W.A. (1996). Structural analysis of substrate binding by the molecular chaperone DnaK. Science *272*, 1606–1614.

Zou, J., Guo, Y., Guettouche, T., Smith, D.F., and Voellmy, R. (1998). Repression of heat shock transcription factor HSF1 activation by HSP90 (HSP90 complex) that forms a stress-sensitive complex with HSF1. Cell *94*, 471–480.

